Electronic Supplementary Information

Facile solvothermal synthesis of $Pt_{76}Co_{24}$ nanomyriapods for efficient electrocatalysis

Liu-Ying Jiang, Xian-Yan Huang, Ai-Jun Wang, Xin-Sheng Li, Junhua Yuan, Jiu-Ju Feng*

College of Chemistry and Life Science, College of Geography and Environmental Science, Zhejiang Normal University, Jinhua, 321004, China

**Corresponding author: jjfeng@zjnu.cn (J. J. Feng).*

Experimental

1. Chemicals

Cetyltrimethylammonium chloride (CTAC), $Pt(acac)_2$, $Co(acac)_3$, *L*-glutamic acid, oleylamine (OAm), commercial Pt/C (20 wt.%) and Pt black (>99.9%) were supplied from Aladdin Chemical Reagent Company (Shanghai, China). The other chemicals were of analytical grade and used without further purification. All of the aqueous solutions were prepared with twice-distilled water throughout the whole experiments.

2. Characterization

The morphology of the samples was characterized by transmission electron microscopy (TEM), high-resolution transmission electron microscopy (HRTEM), high-angle annular dark-field scanning transmission electron microscopy (HAADF-STEM) and energy-dispersive X-ray spectroscopy (EDS) on a JEM-2100F microscope operated at an acceleration voltage of 200 kV. X-ray photoelectron spectroscopy (XPS) measurements were performed on a Thermo VG ESCALAB 250 spectrometer attached with an Al Ka X-ray radiation (1486.6 eV photons) for excitation at 120 W. X-ray diffraction (XRD) spectra were acquired on a Philips PW3040/60 diffractometer using Cu Ka radiation source (l ¼ 0.15405 nm).

3. Electrochemical experiments

All the electrochemical measurements were carried out with a conventional

three-electrode cell at room temperature, where a saturated calomel electrode (SCE) was used as the reference electrode, a platinum wire as the counter electrode, and a modified glassy carbon electrode (GCE, 3 mm in diameter) or a glassy carbon rotating disk electrode (RDE, 3 mm in diameter) as the working electrode.

Meanwhile, oxygen reduction reaction (ORR) measurements were performed by linear sweep voltammetry (LSV) in O_2-saturated 0.1 M $HClO_4$ with a Model 616 RDE. The electrolyte was bubbled with oxygen for 0.5 h before each experiment and maintained over the electrolyte during the whole measurements. The hydrogen evolution reaction (HER) measurements were recorded in N_2-saturated 0.5 M H_2SO_4 and the whole experiments were operated in the nitrogen-saturated electrolyte. All of the experiments were performed at room temperature if not stated otherwise.

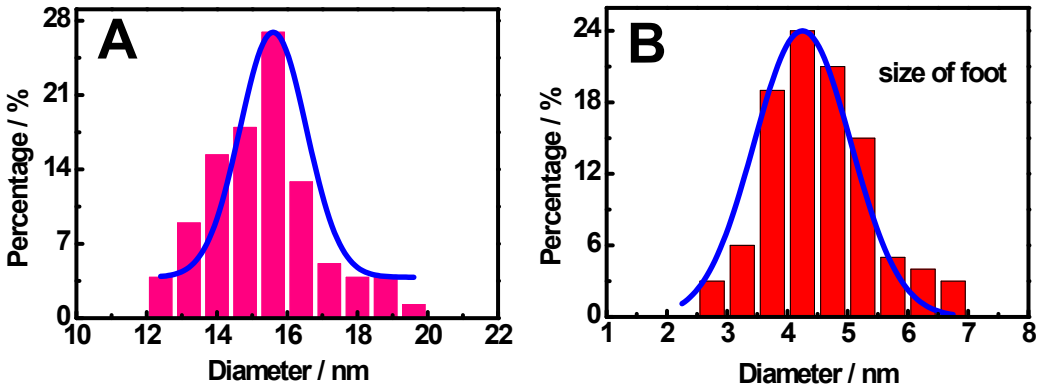

Fig. S1. The size distributions of the (A) whole particle length and (B) foot length.

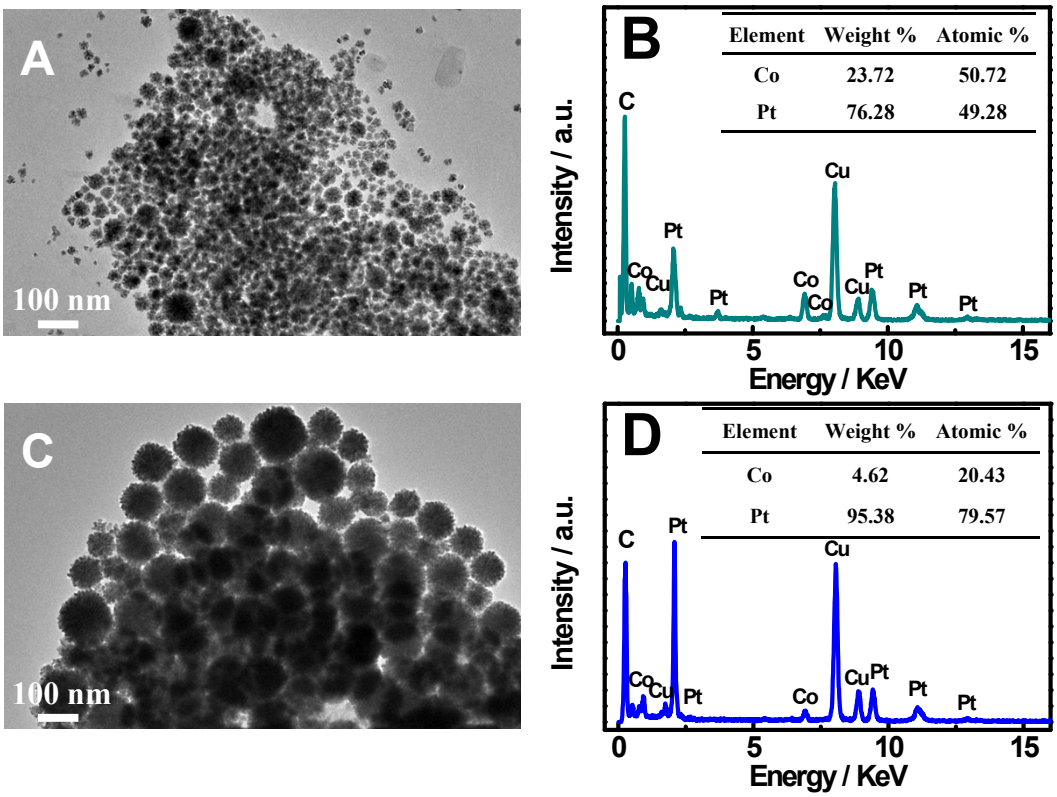

Fig. S2. The TEM images of the PtCo products prepared with different ratios of Pt against Co: (A) $Pt_{49}Co_{51}$ NPs and (C) $Pt_{80}Co_{20}$ NPs. The EDS spectra of (B) $Pt_{49}Co_{51}$ NPs and (D) $Pt_{80}Co_{20}$ NPs.

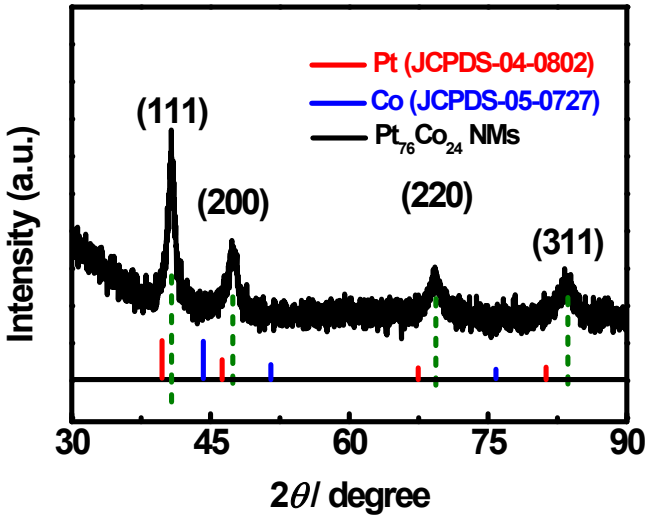

Fig. S3. The XRD pattern of $Pt_{76}Co_{24}$ NMs. Standard XRD spectra of bulk Pt (JCPDS-04-0802) and Co (JCPDS-05-0727) were provided for comparison.

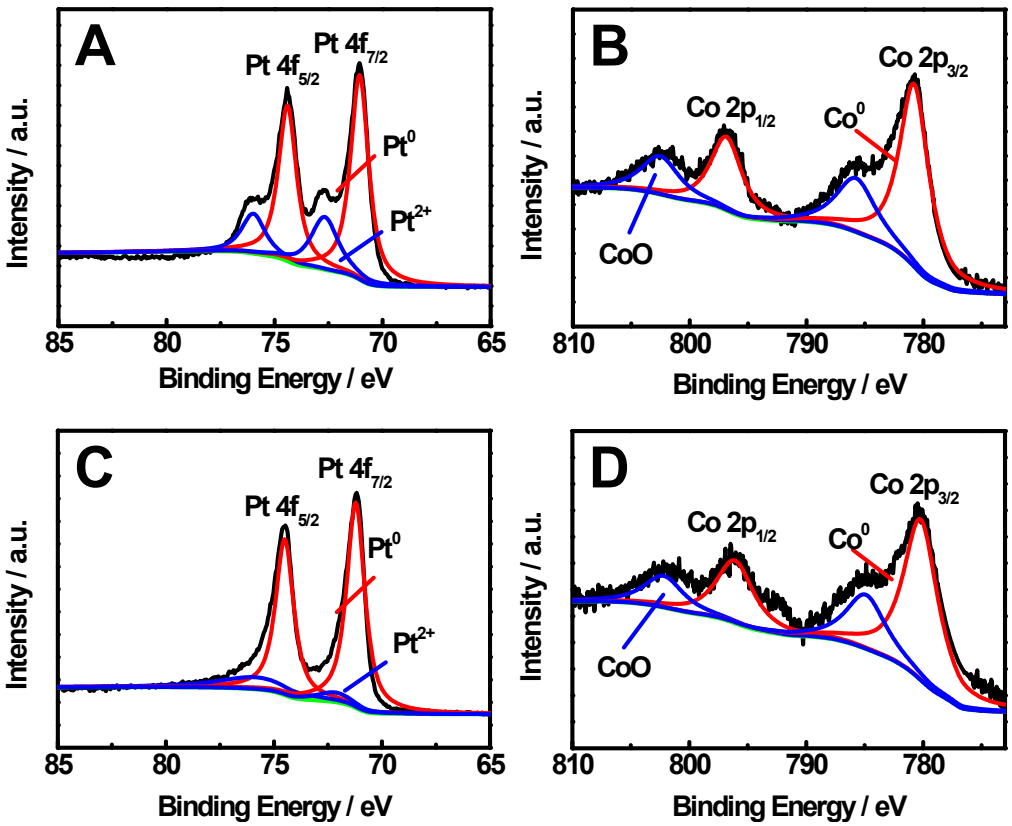

Fig. S4. High-resolution Pt 4f (A, C) and Co 2p (B, D) XPS spectra of $Pt_{49}Co_{51}$ NPs, and $Pt_{80}Co_{20}$ NPs, respectively.

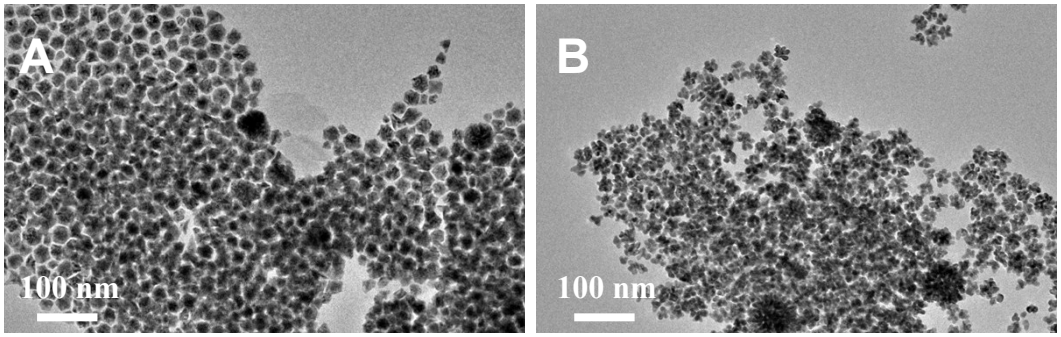

Fig. S5. TEM images of the PtCo products prepared with 5 mM (A) and 35 mM (B) CTAC.

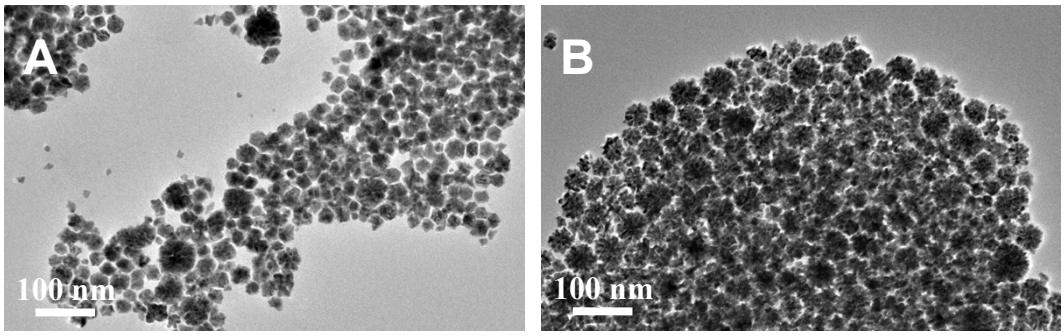

Fig. S6. TEM images of the PtCo products fabricated with 10 mM (A) and 35 mM (B) *L*-glutamic acid.

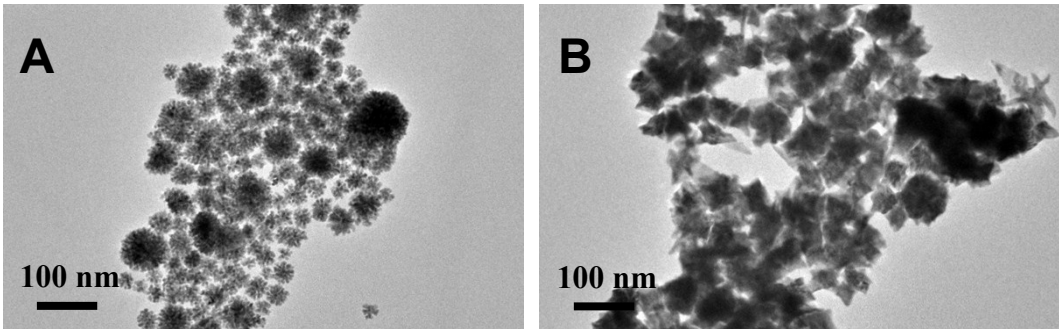

Fig. S7. TEM images of the PtCo products constructed at the reaction temperature of (A) 160 °C and (B) 200 °C.

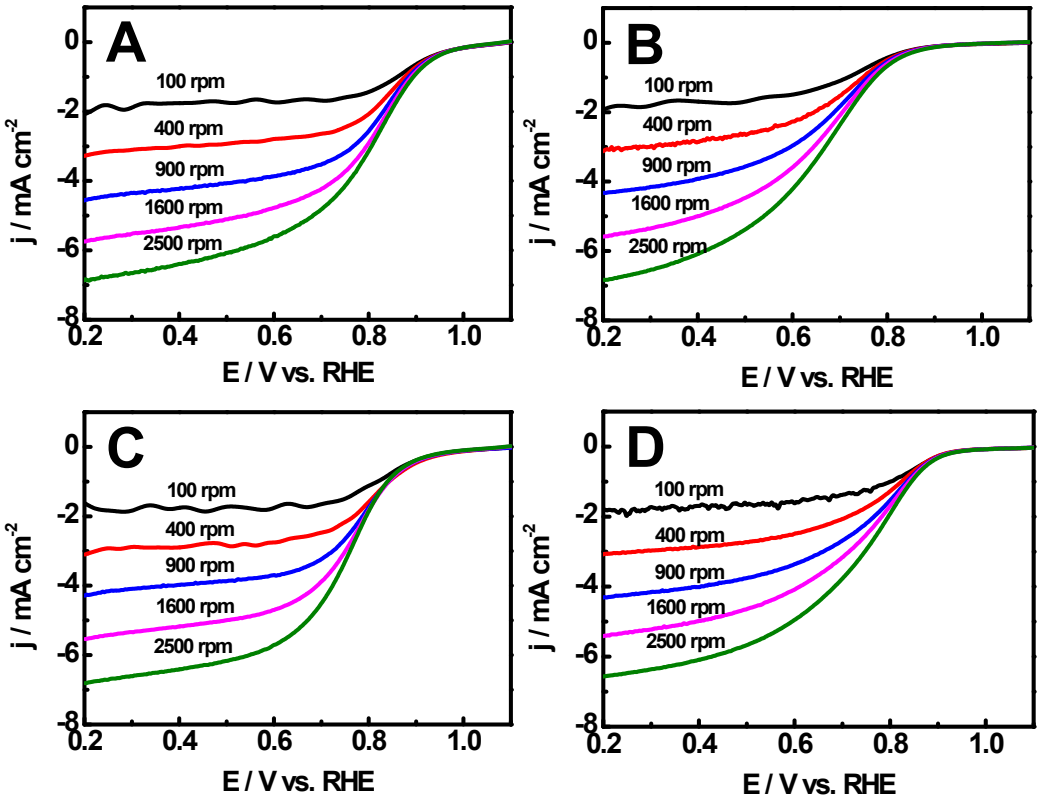

Fig. S8. The LSV curves of (A) $Pt_{76}Co_{24}$ NMs, (B) $Pt_{49}Co_{51}$ NPs, (C) $Pt_{80}Co_{20}$ NPs, and (D) Pt black catalysts in O_2-saturated 0.1 M $HClO_4$ at a scan rate of 5 mV s^{-1} with different rotating rates: 100, 400, 900, 1600, and 2500 rpm.

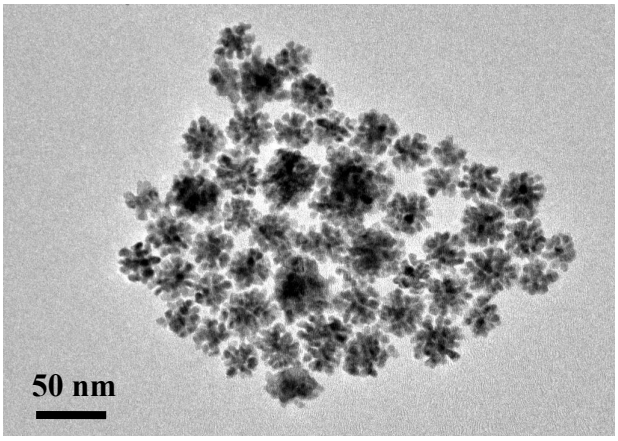

Fig. S9. TEM image of $Pt_{76}Co_{24}$ NMs after 1000 scanning cycles in O_2-saturated 0.1 M $HClO_4$ at a scan rate of 5 mV s^{-1}.

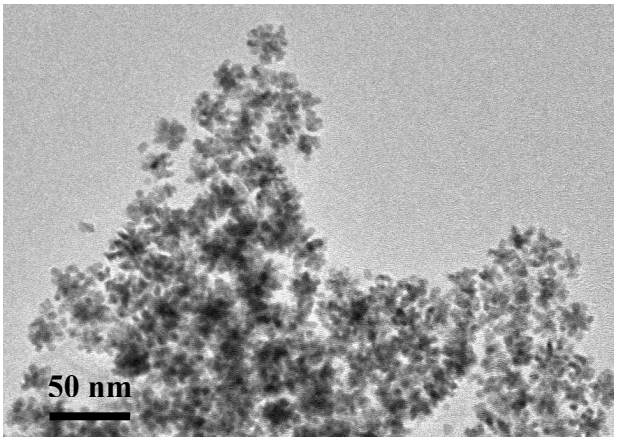

Fig. S10. TEM image of $Pt_{76}Co_{24}$ NMs after 1000 scanning cycles in N_2-saturated 0.1 M H_2SO_4 at a scan rate of 5 mV s^{-1}.

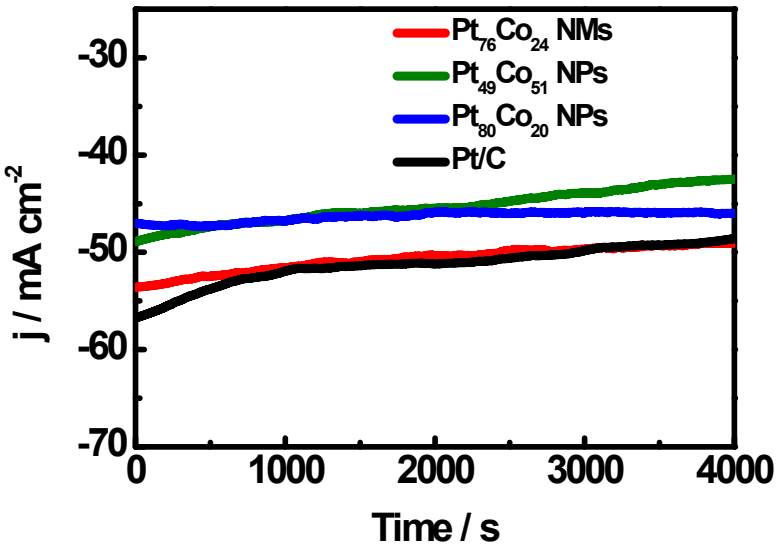

Fig. S11. The chronoamperometric curves of $Pt_{76}Co_{24}$ NMs, $Pt_{49}Co_{51}$ NPs, $Pt_{80}Co_{20}$ NPs and Pt/C catalysts at –0.1 V in 0.5 M H_2SO_4.

Table S1. Comparison of the HER performances in the acid electrolytes with different catalysts.

Catalysts	E_{onset} (mV *vs.* RHE)	Tafel slopes (mV dec^{-1})	References
Pt-TiS_2	-	40.6	[1]
Au-MoS_2	-220	86	[2]
Au NPs-CN_x	-120	72	[3]
Au-aerogel-CN_x	-30	53	[3]
Ni_2P	-	134	[4]
FeCo@NCNTs-NH	-70	74	[5]
NiAu/Au core/shell	-70	36	[6]
Pt/CFs	-	97.8	[7]
Pt/MoS_2/CFs	-	53.6	[7]
PtNiCu	-	28	[8]
$Pd_{3.02}Te$ NWs/rGO	-	63	[9]
$Pt_{76}Co_{24}$ NMs	-31	32	This work

References

1. Z. Zeng, C. Tan, X. Huang, S. Bao and H. Zhang, *Energy Environ. Sci.*, 2014, **7**, 797-803.
2. Y. Shi, J. Wang, C. Wang, T.-T. Zhai, W.-J. Bao, J.-J. Xu, X.-H. Xia and H.-Y. Chen, *J. Am. Chem. Soc.*, 2015, **137**, 7365-7370.
3. M. K. Kundu, T. Bhowmik and S. Barman, *J. Mater. Chem. A*, 2015, **3**, 23120-23135.
4. E. J. Popczun, J. R. McKone, C. G. Read, A. J. Biacchi, A. M. Wiltrout, N. S. Lewis and R. E. Schaak, *J. Am. Chem. Soc.*, 2013, **135**, 9267-9270.

5. J. Deng, P. Ren, D. Deng, L. Yu, F. Yang and X. Bao, *Energy Environ. Sci.*, 2014, **7**, 1919-1923.

6. H. Lv, Z. Xi, Z. Chen, S. Guo, Y. Yu, W. Zhu, Q. Li, X. Zhang, M. Pan, G. Lu, S. Mu and S. Sun, *J. Am. Chem. Soc.*, 2015, **137**, 5859-5862.

7. D. Hou, W. Zhou, X. Liu, K. Zhou, J. Xie, G. Li and S. Chen, *Electrochim. Acta*, 2015, **166**, 26-31.

8. X. Cao, Y. Han, C. Gao, Y. Xu, X. Huang, M. Willander and N. Wang, *Nano Energy*, 2014, **9**, 301-308.

9. L. Jiao, F. Li, X. Li, R. Ren, J. Li, X. Zhou, J. Jin and R. Li, *Nanoscale*, 2015, **7**, 18441-18445.